

## Characterization of the Element Distribution Within TiN Coatings with SIMS

Thomas Kolber<sup>1</sup>, Kurt Piplits<sup>1</sup>, Leopold Palmethofer<sup>2</sup>, and Herbert Hutter<sup>1,\*</sup>

<sup>1</sup> Institute of Analytical Chemistry, University of Technology Vienna, Getreidemarkt 9/151, A-1060 Vienna, Austria

<sup>2</sup> Institute of Semiconductor and Solid State Physics, Johannes Kepler University Linz, Altenbergerstrasse 69, A-4040 Linz, Austria

**Abstract.** The distribution of the relevant elements within TiN coatings, made with two different physical deposition methods as the conventional dc vacuum arc method and the filtered high current pulsed arc method ( $\Phi$ -HCA) are characterized and finally compared. Despite the rougher surface of the dc-arc produced TiN layer, which is due to accumulated droplets, there is no evidence of different stoichiometric composition of Ti and N on the surface. The interface of the dc-arc produced TiN layer (600 nm) is 10 times wider than the one made with the new filtered high current pulsed arc method (60 nm). However the TiN layer made by  $\Phi$ -HCA shows an inhomogeneous distribution of aluminum and chlorine in the vertical direction, whereas the dc-arc sample is homogeneous. Furthermore, the TiN layer made by  $\Phi$ -HCA shows vertically an obvious local maximum of chlorine at a depth of about 130 nm. This vertical local maximum has an homogeneous distribution in horizontal direction, which means that a thin, chlorine enriched layer has been incorporated inside the TiN layer. Nevertheless, quantification by SIMS shows that aluminum as well as chlorine concentrations of both samples are too low to influence any TiN properties.

**Key words:** TiN; superhard coatings; trace elements; SIMS.

The use of conventional materials in sophisticated applications in manufacturing parts of motors and turbines, in energy production, as well as in the production of classical machine tools and medical surgical tools, is no longer adequate to meet the drastically increased technical, economic and ecological demands of new products. For this reason, it

was necessary to improve the surface properties. One attempt to reach this goal is to cover the surface with a compound that meets all technical requirements.

Therefore two new techniques, physical vapor deposition (PVD) and chemical vapor deposition (CVD) [1, 2, 3] have been developed to provide these coatings for industry. One of the established coating technologies in PVD is the vacuum arc source technique, which splits up into different subtypes, such as the conventional dc vacuum arc method or the advanced high current vacuum pulsed arc method. In our investigation, these two techniques have been applied to deposit a TiN coating on silicon substrate. Because of excellent film properties, i.e. extraordinary hardness, a low coefficient of friction and chemical inertness, TiN coatings are successfully applied in different fields of application, such as protection layer on medical prostheses, coatings for metal tools or moving parts under extraordinary conditions (e.g. in guns). In some other fields further development of such layers is still necessary as e.g. satisfactory coatings to protect the teeth have not been developed yet.

The aim of this paper is to characterize and to compare the distribution of the relevant elements within the TiN layers made with the conventional dc-arc vacuum arc technique as well as with the new filtered high current pulsed arc method.

### Experimental

*TiN-Sample, made with dc-arc*

Between a cathode, covered with the material to be evaporated and the anode a low voltage, high current vacuum arc discharge is operated. The arc discharge is concentrated to cathodic spots of a

\* To whom correspondence should be addressed

few microns in diameter and effectively evaporates the target material titanium. Because of high energy density, the evaporated titanium is highly ionized, i.e. in plasma state. This results in effective reactions with the present nitrogen gas atmosphere. An unfavorable feature of vacuum arc based deposition technologies is the emission of macroparticles, originating from cathode spots and flying across the deposition chamber. These so called droplets have dimensions up to tens of micrometers [4] and can easily hit the substrate, which increases surface roughness.

#### *TiN Sample, made with $\Phi$ -HCA*

To achieve smoother surfaces and higher deposition rates, a new type of vacuum arc plasma source, the high current pulsed arc (HCA) was developed [5]. A further improvement of it with complete separation of the droplets from the plasma is the filtered high current pulsed arc method ( $\Phi$ -HCA) [6]. The main steps of plasma production and deposition on the substrate are the same as for the conventional dc-arc method. However the major difference is the use of a pulsed source. This source is arc current, much stronger due to shorter time, which leads to a more homogeneous discharge on the cathode and further to a decrease of the emission probability for droplets. Additionally the  $\Phi$ -HCA has a sectioned filter unit to remove the last few droplets before they reach the substrate surface. Hence less than 15 nm of surface roughness can be achieved with this method.

#### *SIMS Measurement Conditions*

SIMS investigations were performed with a strongly modified CAMECA ims 3f ion microscope [7]. For all measurements an  $O_2^+$  primary ion beam (primary energy: 5.5 kV, primary ion current: 300 nA) was applied to sputter the samples. The depth resolution was limited by the sample surface roughness.

In most cases, a direct measurement of nitrogen with mass 14 is not possible, because of the low sensitivity of  $^{14}N$ . However in our mass spectrum, we detected a rather strong signal at mass 14. To support the assumption that the signal is caused by  $^{14}N$  and not by other ions as  $^{14}C$  or  $^{28}Si^{2+}$ , we moved the primary beam over the sample surface, beginning at a spot with silicon substrate is present without any coating. There the mass spectrum showed one peak at mass 14, which was definitely the signal of  $^{28}Si^{2+}$ . Reaching the area, partly covered with TiN, a second peak at a slightly higher mass than the first peak appeared. Using the high mass resolution mode, the mass difference between those two peaks was determined to be  $\Delta m = 0.016$ , which matches to the mass difference that are calculated with the respective isotope masses. The only ion  $^{14}C$ , that also causes a signal with a similar mass difference to  $^{28}Si^{2+}$  in theory, could not be responsible for this peak, because of the low intensity of its main carbon peak at mass 12. Moving to completely coated areas of the surface, the peak of  $^{28}Si^{2+}$  disappeared, however the other – verified as  $^{14}N$  signal – remained in the mass spectrum.

#### *Depth Measurements*

1D- as well as 3D-SIMS depth profiles actually show the relationship between intensities and cycles. With the aid of aluminum and chlorine implantation standards in TiN substrate as standard samples which are specified later, intensities can be converted into concentrations. To obtain the desired depth information in  $\mu m$ , profile craters are measured with a Dektak IIa profilometer. Therewith the metric depth per cycle can be

obtained by dividing the crater depth by the number of recorded cycles.

## Results and Discussion

### *Direct Imaging Mode*

To obtain a first impression of the distribution of the main elements ( $^{48}Ti$ ,  $^{14}N$ ) and some traces ( $^{27}Al$ ,  $^{35}Cl$ ), we recorded images of the surface in direct imaging mode. Direct imaging mode means that all points of the sample surface can be simultaneously imaged on the detector. The main advantage of this mode is the short measurement time, which allows for real-time viewing of the surface distribution of a selected element. However, the maximum lateral resolution in this mode is  $1 \mu m$ .

The SIMS images for all masses mentioned above are homogeneous for both samples, although the surface of the TiN film obtained with dc vacuum technology shows surface contamination caused by accumulated droplets. These droplets are visible on a respective electron microprobe image (see Fig. 1). Therefore, it can be concluded that no remarkable stoichiometric difference exists between the droplets on the surface and other surface parts.

### *1D-Depth Profile*

To obtain a 1D-depth profile, it is necessary to raster the finely focused primary beam over a square of a common size of about  $150 \mu m$ . The measurement itself takes place in the middle of the square in order to reduce the crater edge effects.

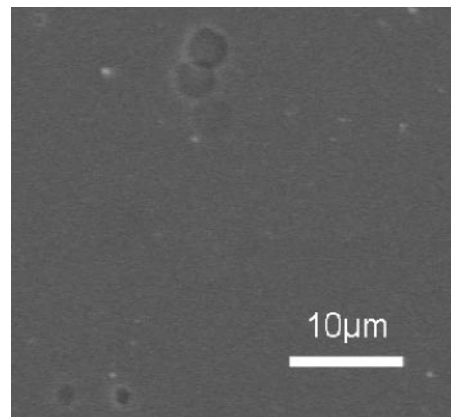
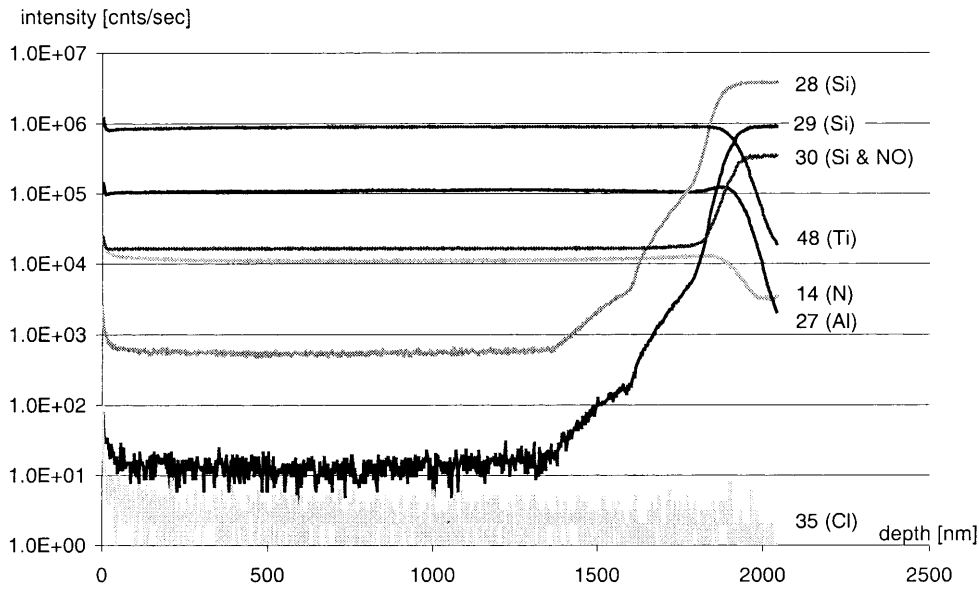
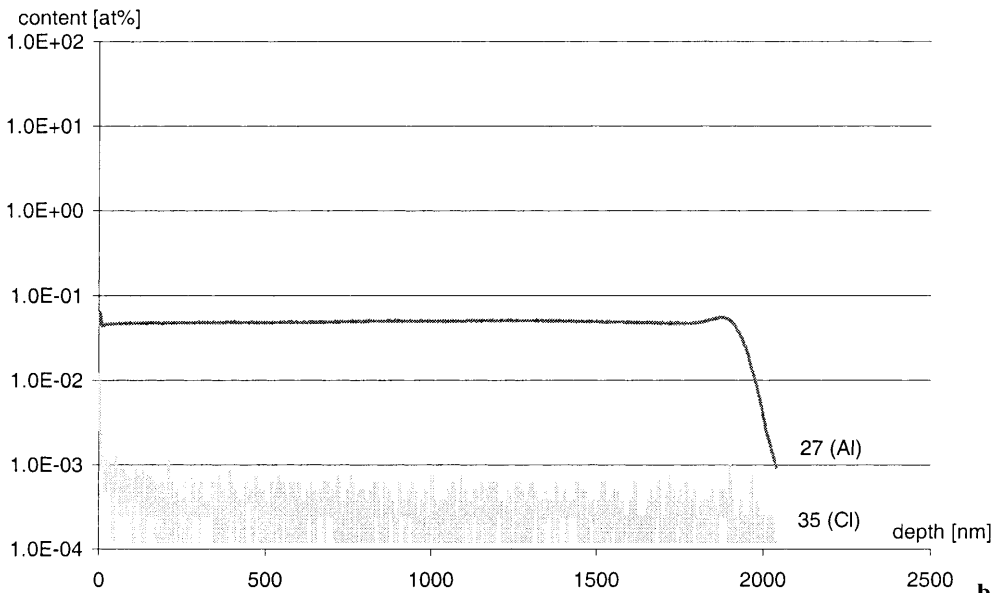


**Fig. 1.** Electron microprobe image (secondary electrons; 20 kV) of the dc-arc TiN layer. The remarkable  $\mu m$ -wide craters are caused by macroparticle impacts (droplets), originating from cathode spots that fly across the deposition chamber



**a**



**b**

**Fig. 2.** SIMS 1D-depth profile of a 1.8  $\mu\text{m}$  thick TiN layer on silicon substrate, made with the dc-arc method (primary ions  $\text{O}_2^+$ , primary current: 300 nA): (a) N, Al, Si, Cl and Ti signals in counts/s; (b) Al and Cl, in at%

In order to obtain representative depth information, we chose three different spots on each sample, where we recorded a 1D-depth profile. The two 1D-depth profiles of each sample show the same result and that supports the assumption that the TiN layer is homogeneous in the horizontal direction. For 1D-

depth profiles, we recorded the signals for the masses  $^{14}\text{N}$ ,  $^{27}\text{Al}$ ,  $^{35}\text{Cl}$  and  $^{48}\text{Ti}$ , which have been found in a mass spectrum before. Additionally we added the signals for the masses  $^{28}\text{Si}$ ,  $^{29}\text{Si}$  and  $^{30}\text{Si}$  to determine the interface area between TiN layer and silicon substrate. The signals for the two less abundant

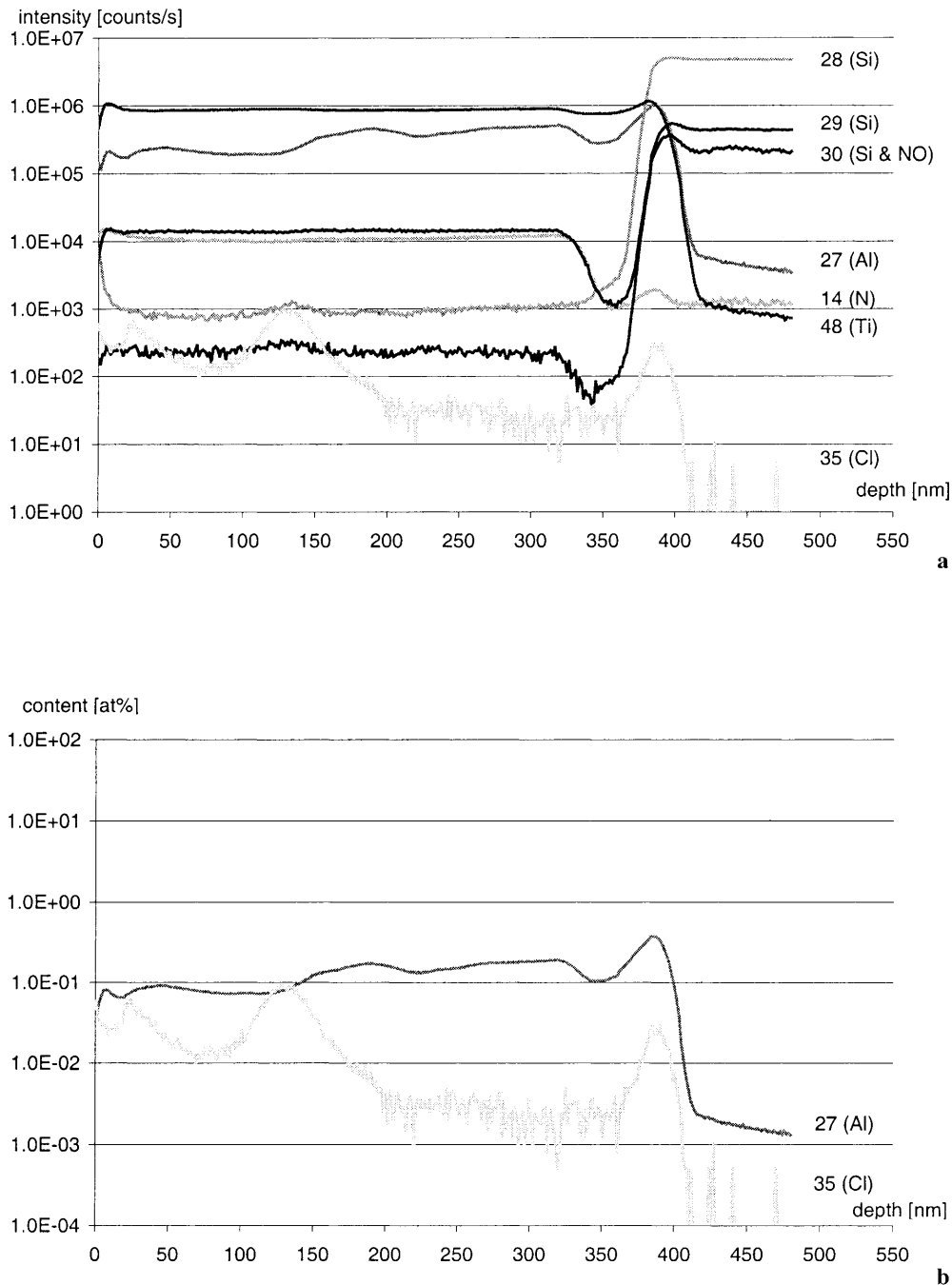


**Fig. 3.** SIMS 1D-depth profile of a 400 nm thick TiN layer on silicon substrate, made with the pulsed high current vacuum arc method (primary ions  $O_2^+$ , primary current: 300 nA): (a) N, Al, Si, Cl and Ti signals in counts/s; (b) Al and Cl in at%

isotopes of silicon –  $^{29}\text{Si}$  and  $^{30}\text{Si}$  – have been added to be sure that the signal at mass 28 is really  $^{28}\text{Si}$  and not a doubly charged iron ion  $^{28}\text{Fe}^{2+}$ . As expected, the parallel slope of the signals for these masses in the interface verifies the mass 28 to be silicon. Inside the

TiN layer, the signal at mass 30 results from  $^{14}\text{N}^{16}\text{O}$ , however, in the silicon substrate from  $^{30}\text{Si}$ .

Looking at the interface of both 1D-depth profiles (see Fig. 2a, 3a), significant differences can be seen. The interface section is the area where the silicon

signal changes. Whereas the dc-arc produced TiN layer shows a rather wide interface of about 600 nm, which will be indicated by the increase of the signal for  $^{28}\text{Si}$  together with the  $^{29}\text{Si}$  signal, the TiN layer produced with the new filtered high current pulsed arc ( $\Phi$ -HCA) shows a distinctly narrower interface of only about 60 nm. This means that the contamination with silicon atoms reaches 10 times deeper inside the TiN layer of the dc-arc produced TiN layer than inside the other. This effect can be explained by droplet formation during dc-arc deposition [4]. These droplets with sizes of tens of micrometers partly dig into the silicon substrate and roughen the surface which was flat before. Further, the 1D-depth profile of the dc-arc sample (see Fig. 2a) shows an homogeneous progress of all elements inside the TiN layer, which means that in vertical direction the concentrations of all investigated elements are constant. However, the 1D-depth profile of the TiN layer produced with the new filtered high current pulsed arc method (see Figure 3a) indicates slight inhomogeneities of aluminum and chlorine in the vertical direction. To be sure about the significance of these traces, quantitative investigations had been carried out.

### SIMS-Quantification with Reference

Quantitative analyses for Al and Cl were carried out with a non-homogeneous ion implantation standard.  $^{27}\text{Al}$ , at a dose of  $5.10^{+15}$  at/cm<sup>2</sup> and  $^{35}\text{Cl}$ , at a dose of  $3.10^{+15}$  at/cm<sup>2</sup> were implanted with an energy of 300 keV into TiN layers on silicon. From the measured depth profile of the respective standard, the RSF for Al as well as for Cl regarding titanium ( $^{48}\text{Ti}$ ) as reference mass was calculated:

$$\text{RSF} = \frac{f_{\text{ref}} \cdot c_{\text{ref}} \cdot \rho \cdot N_A \cdot d}{f_{\text{el}} \cdot Q_T \cdot M \cdot \text{Cyc}} \cdot \sum_{i=1}^{\text{Cyc}} \frac{I_{\text{el}}(i)}{I_{\text{ref}}(i)}$$

$f_{\text{ref}}$	isotope abundance of the reference
$c_{\text{ref}}$	concentration of the reference [at/at]
$\rho$	matrix density [g/cm <sup>3</sup> ]
$N_A$	Avogadro's number ( $= 6.022 \times 10^{23}$ )
$d$	depth of the crater [cm]
$f_{\text{el}}$	isotope abundance of the element
$Q_T$	implanted dose of the element [at/cm <sup>2</sup> ]
$M$	molecular mass of the matrix
$\text{Cyc}$	number of measured cycles
$I_{\text{el}}(i)$	signal intensity for the element [counts/s] of cycle $i$

$I_{\text{ref}}(i)$  signal intensity for the reference [counts/s] of cycle  $i$

With these two sensitivity factors we were able to quantify the respective concentrations of our samples.

The content of aluminum inside the dc-arc TiN layer is about 0,05 at%, whereas the content inside the  $\Phi$ -HCA TiN layer is about 0,15 at% (see Figure 2b and 3b). Nevertheless, both aluminum contents are very small indeed. Similar to aluminum, the content of chlorine inside the  $\Phi$ -HCA TiN layer is higher than the content inside the dc-arc TiN layer. The dc-arc TiN layer shows a homogeneous chlorine distribution with a calculated content of about 0,0005 at%. Because of much higher concentrations of Cl inside the Cl standard, the calculated content is not very accurate but it certainly is at this order of magnitude. However,  $\Phi$ -HCA TiN shows a smaller maximum for chlorine at about 25 nm depth and an obvious local maximum of chlorine at about 130 nm depth. The major peak corresponds with a maximum chlorine concentration of about 0,08 at%, whereas the chlorine concentration of this sample decreases by approximately two orders of magnitude in deeper zones. The reason for the higher chlorine concentrations in  $\Phi$ -HCA TiN layers might lie in the substrate cleaning process performed with acetone, but this has not been completely investigated yet. Nevertheless, these low concentrations of aluminum and chlorine – not only in dc-arc TiN but also in  $\Phi$ -HCA TiN – are probably not sufficient to induce property changes of TiN layers, at least no influences have been found yet.

### 3D-Depth Profile

Although we have recorded 1D-depth profiles of the TiN layer produced with the new filtered high current pulsed arc method at three different locations with the same result, we wanted to be sure not to measure particular inhomogeneities. Therefore, we also recorded a 3D-depth profile of this layer to directly visualize the horizontal distribution of chlorine around the peak maximum at about 13 nm depth.

The observed surface area was  $300 \times 300 \mu\text{m}$ . During a 3D-depth profile recording, secondary ion images of the surface as obtained in the direct imaging mode, are registered using a CCD camera system in combination with a double micro-channel-plate-phosphor screen assembly. The higher the channel-plate high voltage (cphv), the higher the intensity of the channel-plate signal. To avoid destruction of the

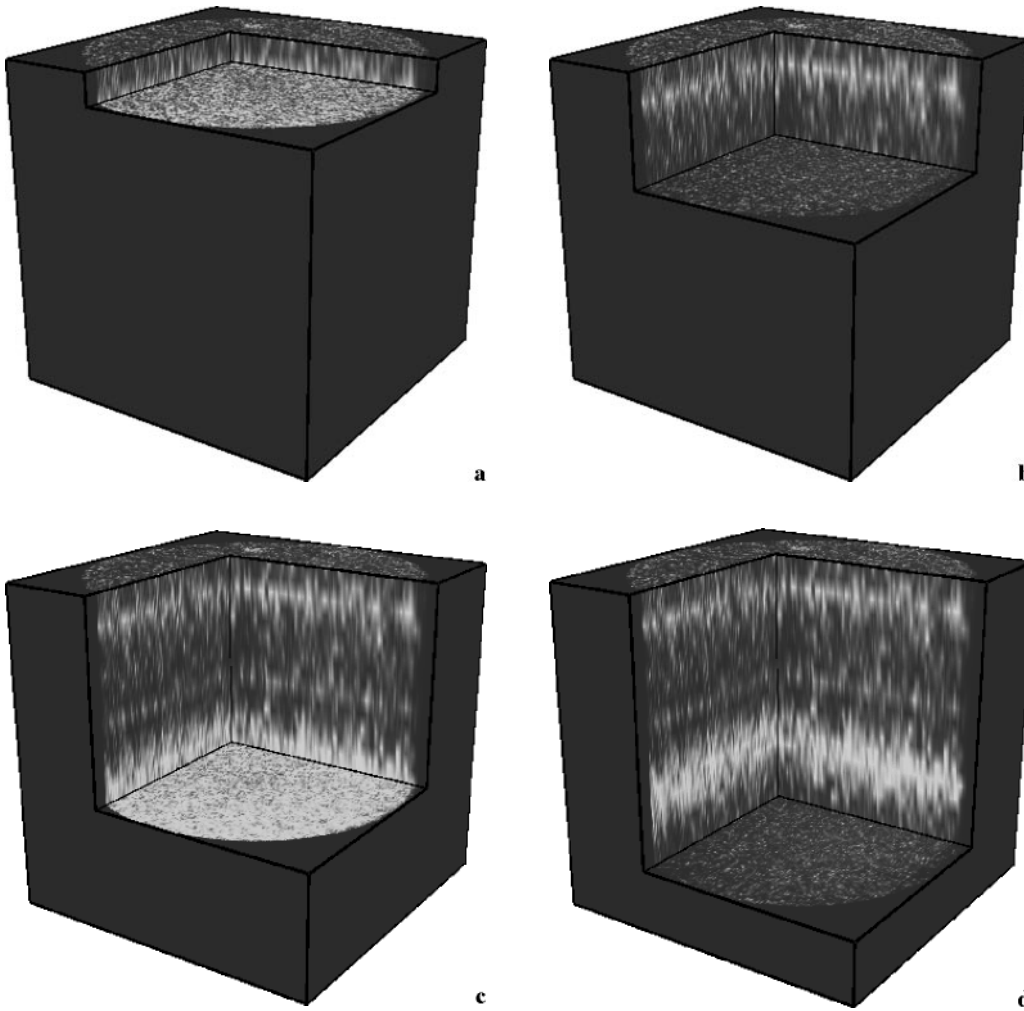


**Fig. 4.** SIMS 3D-depth profiles for  $^{35}\text{Cl}$  of a 400 nm thick TiN layer on silicon substrate, made with the pulsed high current vacuum arc method (primary ions  $\text{O}_2^+$ , primary current: 300 nA, area  $300 \times 300 \mu\text{m}$ ): (a) 25 nm depth; (b) 70 nm depth; (c) 130 nm depth; (d) 160 nm depth

channel-plate by too high intensities, it is necessary to monitor the channel-plate signal intensity automatically. If the intensity reaches a critical value, the cphv will be lowered immediately. On the other hand, if intensities are very low, the system automatically increases the cphv so as to increase the channel-plate intensity. Consequently, the channel-plate provides an image, which uses the full dynamic illumination range independent of the secondary ion intensity. The camera signal is then digitized by an ITI 151 image-processor and stored on the hard disc by the controlling computer.

Data sets for 3D-depth profiles are composed of single images recorded in the direct imaging mode. The single image data are imported and put together

into one big matrix using a self-written C++ computer program called “Visualizer”. This program visualizes the 3D data set in different ways, e.g. as block or in an isosurface representation. To obtain information about the horizontal distribution of chlorine enrichments seen in the respective 1D-depth profile (see Fig. 3), we selected 2 different horizontal cutting planes straight through the smaller and larger chlorine maximum at 25 nm and 130 nm. Additionally, two 3D-depth profiles with cutting planes around the chlorine maximum at 130 nm complete the assumption of a homogeneous lateral distribution of chlorine independent of the depth (see Fig. 4a–d). Therefore, local chlorine contamination can be excluded.

## Conclusion

Despite the rougher surface of the dc-arc produced TiN layer, due to accumulated droplets, there is no evidence of differences in the stoichiometric composition of Ti and N on the surface. Due to droplet formation, the interface of the dc-arc produced TiN layer (600 nm) is 10 times wider than the one of the layer made with the new filtered high current pulsed arc method (60 nm). Furthermore, the TiN layer made by the new filtered high current pulsed arc method shows an inhomogeneous distribution of aluminum and chlorine in the vertical direction, but the dc-arc sample is homogeneous. While the aluminum concentration inside the dc-arc TiN layer is about 0,05 at%, inside the  $\Phi$ -HCA TiN layer it is 0,15 at%. The dc-arc TiN layer shows a homogeneous chlorine distribution with a content of about 0,0005 at%, whereas the  $\Phi$ -HCA TiN layer shows an obvious vertical local maximum of chlorine at about 130 nm depth, which corresponds to a chlorine concentration of about 0,08 at%. Further, the chlorine concentration decreases to 0,003 at% in deeper zones. 3D-SIMS depth profiling shows a homogeneous distribution of chlorine in the horizontal direction also around the

depth of the vertical local maximum at 130 nm. That means, that there is a chlorine enriched layer inside  $\Phi$ -HCA TiN. Nevertheless, the chlorine concentrations of all investigated samples are probably not sufficient to induce property changes of TiN layers.

*Acknowledgements.* The authors gratefully acknowledge financial support of the present work by the Austrian Science Foundation (FWF; Project 12053-CHE). The investigated samples were produced at the Fraunhofer Institute for Material and Beam Technology (IWS), Dresden, Germany.

## References

- [1] M. Andritschky, *Diam. Relat. Mater.* **1995**, 53, 33.
- [2] M. I. Heggie, G. Jungnickel, C. D. Latham, *Diam. Relat. Mater.* **1996**, 5, 236..
- [3] D. T. Quinto, *Diam. Relat. Mater.* **1996**, 14, 7.
- [4] S. Anders, *IEEE T. Plasma Sci.* **1993**, 21, 440.
- [5] P. Siemroth, T. Schülke, T. Witke, *Surf. Coat. Tech.* **1994**, 68/69, 314.
- [6] T. Schülke, A. Anders, P. Siemroth, *IEEE T. Plasma Sci.* **1997**, 25, 660.
- [7] M. Grasserbauer, G. Stinger, G. Friedbacher, A. Virag, *Surf. Interface Anal.* **1989**, 14, 623.

*Received January 3, 2000. Revision April 4, 2000.*